# A Control Approach for Actuated Dynamic Walking in Biped Robots

David J. Braun, *Student Member, IEEE*, and Michael Goldfarb, *Member, IEEE*

***Abstract*—This paper presents an approach for the closed-loop control of a fully actuated biped robot that leverages its natural dynamics when walking. Rather than prescribing kinematic trajectories, the approach proposes a set of state-dependent torques, each of which can be constructed from a combination of low-gain spring–damper couples. Accordingly, the limb motion is determined by interaction of the passive control elements and the natural dynamics of the biped, rather than being dictated by a reference trajectory. In order to implement the proposed approach, the authors develop a model-based transformation from the control torques that are defined in a mixed reference frame to the actuator joint torques. The proposed approach is implemented in simulation on an anthropomorphic biped. The simulated biped is shown to converge to a stable, natural-looking walk from a variety of initial configurations. Based on these simulations, the mechanical cost of transport is computed and shown to be significantly lower than that of trajectory-tracking approaches to biped control, thus validating the ability of the proposed idea to provide efficient dynamic walking. Simulations further demonstrate walking at varying speeds and on varying ground slopes. Finally, controller robustness is demonstrated with respect to forward and backward push-type disturbances and with respect to uncertainty in model parameters.**

***Index Terms*—Biped, dynamic walking.**

## I. Introduction

THE ZERO-MOMENT-POINT (ZMP) approach is perhaps the most comprehensive approach that has been developed in the biped locomotion control literature [1]–[6]. Methods based on this approach have been shown to provide effective, robust, and versatile locomotion for biped robots. Despite their effectiveness, ZMP approaches generally result in a stiff and unnatural-looking gait with low locomotive efficiency [7], [8]. The principal reason that these approaches appear stiff and have a low locomotive efficiency is that they are based on the trajectory tracking and, therefore (by definition), override the natural dynamics of the robot (i.e., position-level information is dictated by the controller, and thus, integration of the inertial dynamics is not an essential part of the motion). Such reshaping of the natural dynamics is energetically expensive. By contrast, humans (which are characterized bynatural-looking gait with high locomotive efficiency) have been shown to leverage the natural dynamics of their limbs when walking (e.g., [9]).

In order to achieve a more efficient and natural-looking bipedal gait, several researchers have investigated dynamic walking approaches that, like humans, leverage rather than override the limb dynamics of the robot. As defined herein, a dynamic walker is one in which the motion of the walker is not dictated substantially by the controller, but rather is influenced significantly by the gravitational and inertial characteristics of the system. As such, neither a predefined reference trajectory nor any other time- or position-based attribute of the walking cycle (i.e., desired walking speed, stepping frequency, or step length) can be enforced by control. Rather, all such gait characteristics are obtained indirectly by the interaction between the dynamics of the robot and environment and the influence of joint torques (i.e., from the combined influences of the joint torques and natural dynamics). Implicit in this definition is that the limb dynamics play a significant role in determining the joint angle trajectories. This definition also implies that the joints should be backdrivable such that power can flow freely and bidirectionally between the limb load and the actuator. Note that the phrase dynamic walking is also used to describe a biped gait that is dynamically (as opposed to statically) stable [10], [11], although this is not the meaning used herein.

Prior work on dynamic walkers includes work on both actuated and unactuated walkers. Specifically, such work describes the development of unactuated (i.e., fully passive) walkers, actuator-assisted walkers that are based largely on passive versions, and actuated walkers that utilize control approaches that do not dictate joint angle trajectories. Fully passive dynamic walkers do not incorporate any actuators (or control), and as such, the locomotion they produce adheres to the previously given definition of dynamic walking (i.e., no motions are imposed by a controller). As such, fully passive dynamic walkers rely on precisely tuned natural dynamics of the robot and must walk on a slight downward slope to compensate for the energetic cost of transport (i.e., they are powered by gravity). Examples of these types of walkers are described in [8], [12], and [13].

Actuator-assisted dynamic walkers augment a nearly passive walker by introducing a reduced set of actuators to overcome the energetic losses associated with gait (i.e., the walkers need not descend a slope) and introduce some robustness to design parameter variation (via some form of feedback control). Examples of actuator-assisted walkers are described in [14]–[16], the latter of which is based, in part, on relevant work presented in [17].

Manuscript received January 30, 2009; revised May 22, 2009. First published August 28, 2009; current version published December 8, 2009. This paper was recommended for publication by Associate Editor K. Yamane and Editor W. K. Chung upon evaluation of the reviewers' comments.

The authors are with the Department of Mechanical Engineering, Vanderbilt University, Nashville, TN 37235 USA (e-mail: david.braun@vanderbilt.edu; michael.goldfarb@vanderbilt.edu).

This paper has supplementary downloadable multimedia material available at http://ieeexplore.ieee.org, provided by the authors. This material, Dynamic Walking Video.wmv, demonstrates the dynamic bipedal walk coordinated by the proposed walking controller. The video can be played with Windows Media Player. The total size is 4.5 MB.

Color versions of one or more of the figures in this paper are available online at http://ieeexplore.ieee.org.

Digital Object Identifier 10.1109/TRO.2009.2028762

A fully actuated, partially dynamic walker is described in [18]–[22]. Specifically, the authors address a reduced-order problem, which maintains balance in the walker by imposing kinematic constraints between several joint angles. In doing so, however, they violate the aforementioned definition of dynamic walking by specifying kinematic constraints. In the work described in [23], a neural network is used to learn the nominal walking trajectories that are generated by an impulsive control approach; then, a proportional–derivative controller is used to enforce these relations as state-dependent constraints. Though the combination of impulsive control followed by passive dynamics is a viable approach to dynamic walking, it is not clear how much of the passive dynamics are preserved through the neural network planner and associated constraint enforcement. Pratt *et al.* [24] present a method that need not override the natural dynamics of the biped (depending on the choice of control parameters). The method described in [24], however, requires some limiting assumptions, namely that the biped feet remain flat on the ground and that the ankle joints remain unactuated (i.e., do not impose torque on the biped). A biologically inspired sensor and motor-neuron-based approach to dynamic walking is described in [25] and [26]. This approach does not utilize a trajectory-tracking objective, but the extent of dynamic walking is unclear, particularly since inertial effects are largely diminished at the scale of implementation and since the joint servos are nonbackdrivable (thus, they preclude bidirectional power flow in the joints, which thus precludes dynamic walking).

This paper presents a control approach that enables fully dynamic biped walking, which can provide a more efficient gait than trajectory-tracking approaches. Rather than prescribing a kinematics (i.e., joint angle trajectories), the approach subjects the robot to a set of state-dependent torques. These torques are constructed from energetically passive elements (i.e., angular springs and dampers with fixed equilibrium points), which influence the natural dynamics to generate a stable gait. Similarly to the approach presented in [24], this paper utilizes the notion of (some) control influences based in the task space. However, the present approach relaxes all assumptions regarding robot configuration (i.e., feet need not be flat on the ground); imposes state-dependent torques generated by low gain spring–damper couples, which are constructed as strictly passive functions with fixed equilibrium points; references some of these torques to an inertial reference frame (IRF) and others to the internal robot frame; and develops a model-based solution to transform the state-dependent control torques to actuator torques that utilize the Gauss principle of least constraint [27], [28].

The proposed control approach, whose application leads to an energy-efficient and natural looking dynamic walk, is described herein and, subsequently, demonstrated via simulation.

## II. Biped Model

The control methodology is based upon a dynamic model of the robot introduced in this section. This model is derived by means of the Gauss principle of least constraint that utilizes the Udwadia–Kalaba approach [29]. Unlike traditionally used biped models that are derived separately for single-support, double-support, and flight phases, the present model offers a unified representation that is valid for all phases of gait. Compared with constrained dynamic formulations that are derived by means of Lagrangian equations of the first kind [30], [31], the approach presented herein provides an analytical description of the biped dynamics under redundant constraints and kinematic singularities and, as such, allows the formulation of a control methodology with no restriction on biped configuration.

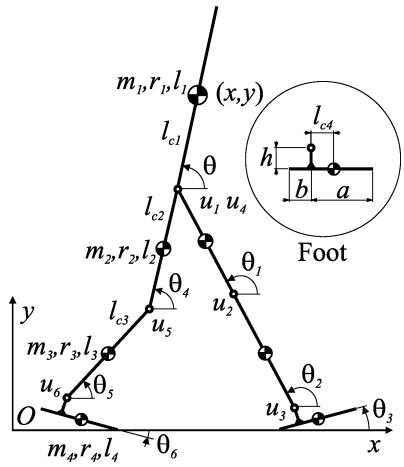


Fig. 1. Seven-link biped with generalized coordinates and associated geometric and inertial properties. The corresponding links on both legs are geometrically and inertially identical. For each segment, the moment of inertia with respect to the center of mass of the associated link is calculated as $I_* = m_* r_*^2$.

In order to facilitate model and controller development, both are developed in the context of a seven-link [9 degrees of freedom (DOFs)] planar biped, as illustrated in Fig. 1. The configuration of the biped is defined with the generalized coordinates, $\mathbf{q} = [x, y, \theta, \theta_1, \theta_2, \theta_3, \theta_4, \theta_5, \theta_6]^T$, which are defined relative to the IRF. The biped is assumed to be actuated at each joint (i.e., right and left hip, knee, and ankle joints), such that the dynamics of the robot are affected by the vector of actuator torques, $\mathbf{u} = [u_1, u_2, u_3, u_4, u_5, u_6]^T$, which are assumed positive in the counterclockwise direction.

### A. Unconstrained Dynamics

Consider an $n$-DOF autonomous multibody system, whose configuration is uniquely specified by $\mathbf{q} \in \Re^n$ generalized coordinates. The equations of motion, for the unconstrained "flying" biped, can be written as

$$\mathbf{M}(\mathbf{q})\ddot{\mathbf{q}} + \mathbf{h}(\mathbf{q}, \dot{\mathbf{q}}) + \mathbf{G}(\mathbf{q}) = \mathbf{Q}_u \tag{1}$$

where $\mathbf{M} \in \Re^{n \times n}$ is a symmetric and positive-definite mass matrix, $\mathbf{h} \in \Re^n$ represents the normal and Coriolis inertial forces, $\mathbf{G} \in \Re^n$ represents the gravitational forces, and $\mathbf{E} \in \Re^{n \times m}$ is a matrix that maps control inputs $\mathbf{u} \in \Re^m$ to generalized control force space $\mathbf{Q}_u = \mathbf{E}\mathbf{u}$. Note that the generalized control force vector $\mathbf{Q}_u$ must belong to the range space of $\mathbf{E}$, $\mathbf{Q}_u \in \mathcal{R}(\mathbf{E})$, which indicates that by using actuator torques $\mathbf{u}$, the motion of the robot in flight phase cannot be fully prescribed. For the biped, all actuator inputs are independent, such that $\text{rank}(\mathbf{E}) = m$.

### B. Kinematic Constraints

Along the walk, the biped is restricted with numerous physical constraints. These kinematic motion restrictions are introduced and discussed as follows.

For the biped in Fig. 1, neither foot can penetrate the ground, the knee joints cannot extend beyond the fully straight position, and both feet are assumed not to slide when in contact with the ground. Since each toe and heel are independently characterized by nonpenetration and no-slip constraint with the ground, the biped dynamics can be subject to ten (dependent) kinematic constraints. Along the walk, the kinematic constraints are "active" when they are imposed on the robot and "inactive" when they do not affect the motion. For each (independent) active constraint, the model loses 1 DOF. For example, when the biped is in single-support phase, with the stance leg foot flat on the ground, three independent constraints are active, which are the nonpenetration of the toe, the nonpenetration of the heel, and one no-slip condition, and as such, the biped is reduced to a 6-DOF system (assuming that neither knee is fully extended). Following a general notation, the set of kinematic constraints imposed on the biped is given by

$$\boldsymbol{\Phi} = [\boldsymbol{\Phi}_h(\mathbf{q})^T, \boldsymbol{\Phi}_n(\mathbf{q}, \dot{\mathbf{q}})^T]^T = \mathbf{0} \tag{2}$$

where $\boldsymbol{\Phi}_h$ represents the holonomic constraints (e.g., the nonpenetration between the toe and heel and the ground, and the full extension of the knee joint), and $\boldsymbol{\Phi}_n$ represents the nonholonomic constraints (i.e., the no-slip condition between each foot and the ground).

We assume that $\boldsymbol{\Phi}_h$ is twice and $\boldsymbol{\Phi}_n$ is at least once differentiable, while the initial conditions are constraint-consistent. In this case, (2) can be equivalently represented as

$$\mathbf{A}(\mathbf{q})\ddot{\mathbf{q}} = \mathbf{b}(\mathbf{q}, \dot{\mathbf{q}}) \tag{3}$$

where $\mathbf{A} = [\mathbf{A}_h^T, \mathbf{A}_n^T]^T$ is the constraint matrix defined in terms of $\mathbf{A}_h = \partial\boldsymbol{\Phi}_h/\partial\mathbf{q}$, $\mathbf{A}_n = \partial\boldsymbol{\Phi}_n/\partial\dot{\mathbf{q}}$, and $\mathbf{b} = \mathbf{A}\ddot{\mathbf{q}} - [\ddot{\boldsymbol{\Phi}}_h^T, \dot{\boldsymbol{\Phi}}_n^T]^T$ [32]. Note that when a constraint becomes inactive (as a function of system configuration), it is eliminated by zeroing the corresponding row in (3). On the other hand, when a constraint switches from inactive to active state (e.g., at the ground contact events or when the knee hits a full extension stop), engagement of the constraint will impart an impact to the system dynamics. The following section describes the treatment of these impact events.

### C. Modeling Impact

For the biped robot, impact occurs when the knee joint fully extends, as well as when each foot impacts the ground. Each impact is considered to be instantaneous and perfectly plastic. With these assumptions, and by defining the pre- and postimpact velocities as $\dot{\mathbf{q}}^-$ and $\dot{\mathbf{q}}^+$, respectively, the postimpact kinematic constraints can be written as

$$\mathbf{A}_h\dot{\mathbf{q}}^+ \geq \mathbf{0}, \qquad \mathbf{A}_n\dot{\mathbf{q}}^+ = \mathbf{0}. \tag{4}$$

Given the no-slip assumption, we will utilize the Gauss principle of least constraint [28], [33] to formulate the effect of the impact as a constrained quadratic minimization problem as follows:

$$\dot{\mathbf{q}}^+ = \min\{\dot{\mathbf{q}} \in \Re^n : (\dot{\mathbf{q}} - \dot{\mathbf{q}}^-)^T\mathbf{M}(\dot{\mathbf{q}} - \dot{\mathbf{q}}^-) \quad \mathbf{A}_h\dot{\mathbf{q}} \geq \mathbf{0}, \mathbf{A}_n\dot{\mathbf{q}} = \mathbf{0}\}. \tag{5}$$

Note that motion restriction in the tangential direction $\mathbf{A}_n\dot{\mathbf{q}} = \mathbf{0}$ is active only if a particular constraint does not break; however, (5) neglects the tangential velocity component, even if a corresponding constraint breaks. This assumption, which cannot be used under "fast" impulsive rebound, becomes reasonable under "slow" nonimpulsive constraint detachment. Practically, when bipedal walking is considered, both the knee and foot are expected to detach nonimpulsively (and nearly normal to the constraint manifold), which justifies the use of (5). Compared with more general considerations [34]–[38], (5) is particularly well suited to the present context, in that it does not require computation of physical constraint forces, which may not be possible under redundant constraints and kinematic singularities.

### D. Constrained Dynamics

Based on the Gauss principle of least constraint [27], [29], [39], the constrained acceleration $\ddot{\mathbf{q}}$, which satisfies (3), can be obtained from the following quadratic programming problem:

$$\ddot{\mathbf{q}} = \min\{\mathbf{x} \in \Re^n : (\mathbf{x} - \mathbf{a})^T\mathbf{M}(\mathbf{x} - \mathbf{a}), \mathbf{A}\mathbf{x} = \mathbf{b}\} \tag{6}$$

where $\mathbf{a} = \mathbf{M}^{-1}(\mathbf{Q}_u - \mathbf{h} - \mathbf{G})$ is the unconstrained acceleration [i.e., the acceleration the system would have without the imposed constraints (3)]. According to (6), $\ddot{\mathbf{q}}$ minimizes the acceleration energy $(\ddot{\mathbf{q}} - \mathbf{a})^T\mathbf{M}(\ddot{\mathbf{q}} - \mathbf{a})$ between the motion that is not restricted with the kinematic constraints and the constrained motion. Since $\mathbf{M}$ is symmetric and positive-definite, the aforementioned quadratic programming problem is convex, and the solution of (6), i.e., $\ddot{\mathbf{q}} = \mathbf{a} + \mathbf{M}^{-1}\mathbf{A}^T(\mathbf{A}\mathbf{M}^{-1}\mathbf{A}^T)^{-1}(\mathbf{b} - \mathbf{A}\mathbf{a})$, exists and is unique. In cases in which $\mathbf{A}$ is not full-rank (which is often the case in a walking biped), $(\mathbf{A}\mathbf{M}^{-1}\mathbf{A}^T)^{-1}$ will not exist. In such cases, we can find the constrained acceleration $\ddot{\mathbf{q}}$ from

$$\ddot{\mathbf{q}} = \mathbf{a} + \mathbf{R}^{-1}\mathbf{C}^+(\mathbf{b} - \mathbf{A}\mathbf{a}) \tag{7}$$

where $\mathbf{R}$ is defined as the upper triangular Cholesky factorization of the mass matrix $\mathbf{M} = \mathbf{R}^T\mathbf{R}$ [40], $\mathbf{C} = \mathbf{A}\mathbf{R}^{-1}$ is the inertially weighted constraint matrix, and $\mathbf{C}^+$ is the pseudoinverse (i.e., the Moore–Penrose inverse) of $\mathbf{C}$ [41]. This formulation explicitly defines the acceleration of the constrained motion, which is well defined under dependent constraints. Note that (7) is expressed using the Cholesky factorization of the mass matrix $\mathbf{R}$ instead of its principal square root $\mathbf{M}^{1/2}$ that is utilized by Udwadia and Kalaba [29], [32].

The Gauss principle of least constraint is valid for any rigid-body system subjected to "ideal" constraints. Accordingly, due to the no-slip assumption, all constraints in the biped [introduced by (2)] are ideal, and as such, (7) provides a viable equation of motion that is used in the following control design.

## III. Control Approach for Dynamic Walking

In this section, we develop a control methodology that can be used to generate dynamic walking in legged robots.

### A. Guideline for Control Torque Selection

Instead of directly using the actuator torques $\mathbf{u}$, we introduce here the desired generalized control forces $\mathbf{Q}_d \in \Re^n$ to control the biped motion. This new control element, which will be used to directly apply torques between the robot and the IRF, is shown to simplify control design, and this makes control parameter selection intuitive. Realization of $\mathbf{Q}_d$ using actuator torques $\mathbf{u}$ is discussed in the next section.

Our objective in walking is to maintain an upright body position and also to sustain a stable oscillation in leg motion that is characterized by a ballistic component in swing. The first objective, which is to maintain an (essentially) upright body position, can be achieved by prescribing a torque that attracts the torso to a nominally vertical position (i.e., in the model coordinates of Fig. 1, a torque that attracts $\theta$ toward an angle at or near $90^\circ$).

In order to drive leg oscillation, the thigh segments are subjected to alternating torques, where the alternation is driven by changes in biped configuration (e.g., heel strike and heel off). Specifically, during swing phase, the prescribed torque drives hip flexion by attracting the thigh segment toward a given (flexion) angular orientation. Upon heel strike, another torque drives hip extension by attracting the thigh segment toward a given (extension) angular orientation.

During swing, the knee is not subject to a driving torque, but rather is subject only to damping. During early stance phase (i.e., heel strike to heel off), a somewhat stiff spring maintains the knee in an extended position. Note that a less stiff spring could be utilized to encourage stance knee flexion; however, walking with a straight leg in (most of) stance is described here, since doing so may reduce knee actuator torque and power requirements. Further, as is recognized through numerous simulation experiments, a "locking" knee enhances the basin of attraction for a stable gait limit cycle. The ankle is subject to a torque during swing that encourages slight flexion (to prevent stumbling) and to one during stance that generates a slight push-off before the stance leg enters swing.

Note that the torso and the thigh segment torques are defined relative to the IRF, while the knee and ankle torques are defined relative to the respective adjacent links. That the torso torque would be defined relative to the IRF is perhaps obvious, since gravity is assumed fixed with respect to the IRF, and postural stability is relevant only when it is defined with respect to the gravity vector. Referencing the thigh segment torques with respect to the IRF (as opposed to the torso) is less obvious, but achieving a desired (angular) dynamics with respect to the inertial frame is recognized as simpler than commanding torques with respect to the moving links in the nonlinearly coupled system.

It is important to mention that the control torques either referenced to the inertial frame or defined on the robot frame influence only the rotational dynamics of the robot. One does not need to apply forces that influence the vertical or horizontal dynamics of the torso, since the upper body will be carried atop the legs, and thus, the appropriate horizontal and vertical motion will be dictated by the motion of the lower limbs.

As described, we do not specify any trajectories in time or space but only define a single attraction point for each state. By utilizing torques that are defined in this manner, we attract the biped toward a desired configuration but do not dictate the path by which it arrives (in time or in space). Moreover, the controller does not attempt to directly maintain a desired forward speed, step frequency, or stride length; rather, these motion attributes are obtained as a result of the interaction between the natural dynamics of the robot and the low-gain controller.

### B. Transforming the Desired Control Torques to the Actuator Space

As described in the previous section, the control problem is made more intuitive by referencing thigh and torso torques to the inertial coordinate frame, while knee and ankle torques are defined relative to adjacent links. In order to implement the presented approach, we propose a transformation between the desired generalized control forces, $\mathbf{Q}_d$ (introduced in the previous section), and the actuator torques $\mathbf{u}$ as follows.

The objective of the transformation is to achieve the same constrained motion that forces the dynamics (7) with $\mathbf{Q}_u = \mathbf{E}\mathbf{u}$ as would be achieved with the application of $\mathbf{Q}_d$. Denoting the desired constrained acceleration as $\ddot{\mathbf{q}}_d$ (generated by $\mathbf{Q}_d$) and the constrained acceleration generated by the actuator torques as $\ddot{\mathbf{q}}$, the objective of the transformation can be stated as $\ddot{\mathbf{q}} = \ddot{\mathbf{q}}_d$. In order to consider this equivalence further, we must first consider issues of overactuation and underactuation.

*1) Overactuation and Underactuation of the Constrained Dynamics:* Due to the presence of the kinematic constraints (2), the biped could, at times, be fully actuated (i.e., same number of actuators as unconstrained DOFs), overactuated (i.e., more actuators than unconstrained DOFs), or underactuated (fewer actuators than unconstrained DOFs). For example, the biped will be fully actuated when in single-support phase and when the foot is flat on the ground. The biped will be overactuated in the double-support configuration. Finally, the robot will be underactuated when two or fewer (independent) constraints are active, such as when in single-support phase and only a single toe or heel (and nothing else) is in contact with the ground.

In order to address the issue of underactuation, we characterize the effect of the control force on the constrained motion of the biped. Let us first segment the unconstrained acceleration $\mathbf{a}$ as follows:

$$\mathbf{a} = \mathbf{a}_0 + \mathbf{a}_u = -\mathbf{M}^{-1}(\mathbf{G} + \mathbf{h}) + \mathbf{M}^{-1}\mathbf{Q}_u \tag{8}$$

where $\mathbf{a}_0$ is the unconstrained acceleration generated by the uncontrolled dynamics, and $\mathbf{a}_u = \mathbf{M}^{-1}\mathbf{Q}_u$ is the unconstrained acceleration that results from the actuator torques. By substituting (8) into (7) provides a similar relation for the constrained accelerations

$$\ddot{\mathbf{q}} = \ddot{\mathbf{q}}_0 + \ddot{\mathbf{q}}_u = \mathbf{R}^{-1}\mathbf{C}^{+}\mathbf{b} + \mathbf{R}^{-1}(\mathbf{I} - \mathbf{C}^{+}\mathbf{C})\mathbf{R}\mathbf{a}_0 + \mathbf{R}^{-1}(\mathbf{I} - \mathbf{C}^{+}\mathbf{C})\mathbf{R}\mathbf{a}_u \tag{9}$$

where $\ddot{\mathbf{q}}_0$ [the first two terms on the right-hand side of (9)] is the constrained acceleration that results from the uncontrolled dynamics, whereas $\ddot{\mathbf{q}}_u$ is the constrained acceleration that is directly related to the generalized control forces, and $\mathbf{I} \in \Re^{n\times n}$ is an identity matrix. By substituting $\mathbf{a}_u$ from (8) into (9), we can obtain the explicit relation of $\ddot{\mathbf{q}}_u$ in terms of the generalized control forces $\mathbf{Q}_u$

$$\ddot{\mathbf{q}}_u = \mathbf{R}^{-1}\mathbf{N}\mathbf{R}^{-T}\mathbf{Q}_u \tag{10}$$

where $\mathbf{N} = \mathbf{I} - \mathbf{C}^{+}\mathbf{C} \in \Re^{n\times n}$ is a symmetric projection operator to the null space of the inertially weighted constraint matrix $\mathbf{C}$. Active constraints will reduce the biped DOFs, which are given by $n_c = \text{rank}(\mathbf{N}) \leq n$. Active constraints can also reduce the effect of the control inputs. For the generalized control forces $\mathbf{Q}_u = \mathbf{E}\mathbf{u}$ in (10), the number of control inputs that can independently alter the constrained motion is given by $m_c = \text{rank}(\mathbf{N}\mathbf{R}^{-T}\mathbf{E}) \leq m$.

The type of actuation for the constrained dynamics can now be defined. If $n_c = m_c$, the number of DOFs for the constrained motion is equal to the number of independent control actuators, and as such, the system is said to be fully actuated. In this case, the transformation between the desired dynamics and achievable dynamics is exact. If $n_c < m_c$, the biped has more independent actuators than active DOFs, and the system is said to be overactuated. In this case, $\mathbf{u}$ is not unique (i.e., the desired dynamics can be reproduced with different control inputs). Finally, in the case when $n_c > m_c$, the system is underactuated, and as such, the desired dynamics cannot, in general, be achieved.

*2) Transformation in a Fully Actuated and Overactuated Configuration:* Since the control input affects only the controlled part of the constrained acceleration (10), the equivalence relation between the desired and actual motion ($\ddot{\mathbf{q}} = \ddot{\mathbf{q}}_d$) can be written as

$$\mathbf{R}^{-1}\mathbf{N}\mathbf{R}^{-T}\mathbf{E}\mathbf{u} = \mathbf{R}^{-1}\mathbf{N}\mathbf{R}^{-T}\mathbf{Q}_d. \tag{11}$$

Note that this relation defines $n$ (possibly dependent) equations with $m$ unknown control inputs $\mathbf{u}$, where the degree of dependence is a function of the constraint configuration $\mathbf{N}$. Utilizing the generalized inverse notation [41], a particular solution to (11) for the actuator torque vector is given by

$$\mathbf{u} = (\mathbf{R}^{-1}\mathbf{N}\mathbf{R}^{-T}\mathbf{E})^{+}\mathbf{R}^{-1}\mathbf{N}\mathbf{R}^{-T}\mathbf{Q}_d. \tag{12}$$

The solution defined by this relation exists regardless of over- or underactuation, although it does not necessarily satisfy (11). Practically, if the system is fully actuated, then $\mathbf{u}$ is a unique solution of (11). In the overactuated case, there is no unique solution of (11). In this case, (12) provides a solution of (11) in the minimum squared Euclidean norm sense (i.e., $\mathbf{u}^T\mathbf{u} \rightarrow$ min). If, however, the system is underactuated, (11) cannot be solved exactly, and as such, (12) defines $\mathbf{u}$, which minimizes the squared Euclidean norm of the difference between the desired and the actual acceleration, i.e., $(\ddot{\mathbf{q}} - \ddot{\mathbf{q}}_d)^T(\ddot{\mathbf{q}} - \ddot{\mathbf{q}}_d) \rightarrow$ min. Note, however, that $\mathbf{q}$ contains both translational and rotational coordinates, and as such, in the uncontrollable case, the control solution is not dimensionally consistent and does not have a clear physical interpretation [42].

*3) Transformation With Dimensional Consistency:* Motivated by the Gauss principle of least constraint, we embed (11) in the following more general formulation:

$$\mathbf{u} = \min\{\mathbf{u} \in \Re^m : (\ddot{\mathbf{q}} - \ddot{\mathbf{q}}_d)^T\mathbf{M}(\ddot{\mathbf{q}} - \ddot{\mathbf{q}}_d)\}. \tag{13}$$

In contrast to (11), the aforementioned quadratic program will provide physically consistent actuator torque computation even through motion phases that are underactuated with the joint torque actuators.

In the present context, we expect any underactuated phases, if present, to occur only for brief periods (i.e., for periods much shorter than the characteristic times associated with the biped dynamics). As such, we assume any departure in dynamic behavior due to uncontrollability to be small. Now, using (9) and (10), one can express (13) as an explicit quadratic program for $\mathbf{u}$ as

$$\mathbf{u} = \min\left\{\mathbf{u} \in \Re^m : \frac{1}{2}\mathbf{u}^T\mathbf{A}_u^T\mathbf{A}_u\mathbf{u} - \mathbf{b}_u^T\mathbf{A}_u\mathbf{u}\right\} \tag{14}$$

where $\mathbf{A}_u = \mathbf{N}\mathbf{R}^{-T}\mathbf{E}$, and $\mathbf{b}_u = \mathbf{N}\mathbf{R}^{-T}\mathbf{Q}_d$. Considering the fact that $\mathbf{N}$ is, in general, rank-deficient, a particular solution to (14) can be defined as

$$\mathbf{u} = (\mathbf{N}\mathbf{R}^{-T}\mathbf{E})^{+}\mathbf{N}\mathbf{R}^{-T}\mathbf{Q}_d. \tag{15}$$

The solution expressed by (15) is physically consistent for all cases of actuation. Specifically, if the biped is fully actuated (i.e., $n_c = m_c$), (15) yields the solution for $\mathbf{u}$ that yields $\ddot{\mathbf{q}} = \ddot{\mathbf{q}}_d$. In the overactuated case (i.e., $n_c < m_c$), the solution to (15) satisfies the matching dynamics criterion (i.e., $\ddot{\mathbf{q}} = \ddot{\mathbf{q}}_d$) and minimizes the squared Euclidean norm of $\mathbf{u}$. Finally, in the case that the biped is underactuated (i.e., $n_c > m_c$), (15) minimizes the acceleration energy between the desired and the actual motion. Using (15), one can transform the desired generalized control forces $\mathbf{Q}_d$ to actuator torques $\mathbf{u}$. Note that just as in the case of human walking, there is no guarantee that the biped can recover a stable gait limit cycle from any underactuated configuration with the proposed control solution.

*4) Works Related to the Proposed Transformation:* Using quadratic programming, a method was proposed in [43] to modify the predefined reference trajectories to maintain balance while walking. Other works, e.g., [24] and [44], present methods that can be used to transform generalized forces to joint torques. Compared with the presented approach, these methods do not provide a unified control force computation through changing constraints and are restricted with respect to the robot configuration (e.g., at least one foot is assumed flat on the ground).

## IV. Implementation on a Seven-Link Biped

We illustrate and further describe the proposed approach via implementation and simulation on the seven-link biped that is illustrated in Fig. 1.

### A. Choice of Control

In order to define the control actions, we impose seven state-dependent torques that directly alter the rotational dynamics of the biped. Each of these state-dependent torques can be

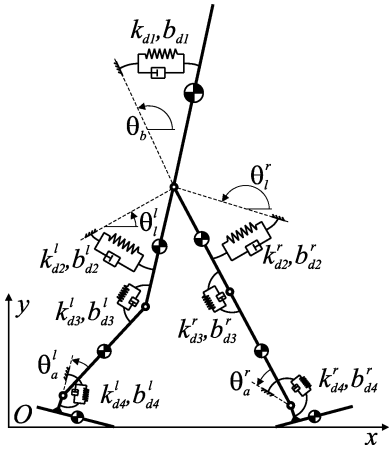


Fig. 2. Schematic representation of the control elements.

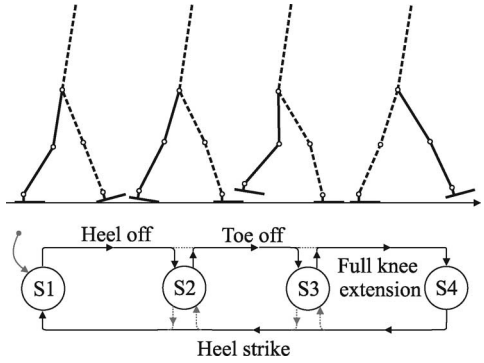


Fig. 3. State-flow diagram. The state flow presented with solid line corresponds to the solid leg along normal walking.

constructed from energetically passive spring–damper couples with fixed equilibrium points. These include an angular torque on the torso with respect to the IRF, state-dependent alternating angular torques on both thighs (also with respect to the IRF), and state-dependent torques on knees and ankles, both with respect to the robot frame (i.e., defined with respect to adjacent links). As such, the vector of desired generalized control forces can be expressed as

$$\mathbf{Q}_d = -\mathbf{K}_d(\boldsymbol{\phi} - \boldsymbol{\phi}_d) - \mathbf{B}_d\dot{\boldsymbol{\phi}} \tag{16}$$

where

$$\mathbf{K}_d = \begin{bmatrix} 0 & 0 & 0 & 0 & 0 & 0 & 0 \\ 0 & 0 & 0 & 0 & 0 & 0 & 0 \\ k_{d1} & 0 & 0 & 0 & 0 & 0 & 0 \\ 0 & k_{d2}^r & -k_{d3}^r & 0 & 0 & 0 & 0 \\ 0 & 0 & k_{d3}^r & -k_{d4}^r & 0 & 0 & 0 \\ 0 & 0 & 0 & k_{d4}^r & 0 & 0 & 0 \\ 0 & 0 & 0 & 0 & k_{d2}^l & -k_{d3}^l & 0 \\ 0 & 0 & 0 & 0 & 0 & k_{d3}^l & -k_{d4}^l \\ 0 & 0 & 0 & 0 & 0 & 0 & k_{d4}^l \end{bmatrix} \tag{17}$$

is the stiffness matrix, $\mathbf{B}_d$ is the matrix of linear damping coefficients [which has the same form as (17)], $\boldsymbol{\phi} = [\theta, \theta_1, \theta_2 - \theta_1, \theta_3 - \theta_2 + \pi/2, \theta_4, \theta_5 - \theta_4, \theta_6 - \theta_5 + \pi/2]^T$ defines the feedback information for the control torque computation, and $\boldsymbol{\phi}_d = [\theta_b, \theta_l^r, 0, \theta_a^r, \theta_l^l, 0, \theta_a^l]^T$ defines the equilibrium point of each spring (i.e., it can be considered as the attraction point of each spring). The parameters that define $\mathbf{Q}_d$ for the seven-link biped are shown schematically in Fig. 2. Note that the right- and left-hand-side parameters are indicated with superscripts.

It should be noted that the control given by (15) and (16) does not guarantee a dynamic walk. Specifically, in order to meet the criteria for dynamic walking, the stiffness and damping parameters of the controller must be selected to be sufficiently low such that the control influence does not substantively prescribe the motion of the robot.

As mentioned previously, leg oscillation is generated by application of alternating torques (defined with respect to the IRF) applied to each thigh segment. This alternation is switched based on an event-driven finite-state structure. As follows, we describe the finite-state logic along which the control parameters $\mathbf{K}_d, \mathbf{B}_d,$ and $\boldsymbol{\phi}_d$ are changed as piecewise constant functions.

Let us start at heel strike that induces application of the state-dependent torques that attract the thigh toward a hip-extension configuration, initiates knee locking with a somewhat stiff spring and damper, and imposes a spring–damper element at the ankle that accumulates elastic energy during stance to provide an ankle push at late stance. The heel-off event (i.e., when the heel leaves the ground) switches the hip torque (equilibrium angle) to one that attracts the thigh toward a hip-flexion configuration and allows the ankle to release the energy accumulated during stance through push-off. In addition to these two states, two additional states are used to facilitate stable locomotion. Specifically, following the toe-off event (when the swing foot is entirely in the air), the swing leg ankle equilibrium point (i.e., angle of attraction) is moved to a slightly flexed position, which enhances ground clearance while the swing knee is only slightly damped. The final state, which is defined when the knee reaches full extension, is used to retain the knee at full extension and, thus, prepare the (extended) swing leg for heel strike. Thus, the gait controller consists of four states, as illustrated in Fig. 3. Note that the states apply independently to each leg and do not apply at all to the torque acting on the torso (i.e., the control parameters for the torso are not changed during the motion). As such (for each leg), state 1 consists of stance, state 2 is initiated by heel-off, state 3 initiated by toe-off, state 4 initiated by full knee extension, and the leg is returned to state 1 by heel strike. Due to external disturbances or other type of uncertainties, however, the described event flow may not remain preserved along the motion of the robot. In this light, the state of each leg is identified based on its constraint configuration (i.e., state 1—both toe and heel on ground; state 2—toe on ground, heel off ground; state 3—both toe and heel off ground; state 4—toe and heel off ground and extended knee on a forward swing leg). In particular, switching from state 3 (swing) to state 1 (stance) is important if, during swing, an incomplete knee extension occurs (which was recognized through the push disturbance simulations presented subsequently). Further cross-switching has also been recognized to improve the robustness of the proposed control methodology.

TABLE I
GEOMETRIC AND INERTIAL PARAMETERS [46]

| Description | no. $(*)$ | $l_*/L$ | $l_{c*}/l_*$ | $m_*/M$ | $r_*/l_*$ |
|---|---|---|---|---|---|
| Upper body | 1 | 0.288 | 0.626 | 0.6780 | 0.496 |
| Thigh | 2 | 0.245 | 0.433 | 0.1000 | 0.323 |
| Shank | 3 | 0.246 | 0.433 | 0.0465 | 0.302 |
| Foot | 4 | 0.152 | 0.250 | 0.0145 | 0.475 |
| Foot geometry | | $a/l_4$ | $b/l_4$ | $h/L$ | |
| | | 0.75 | 0.25 | 0.039 | |

TABLE II
CONTROLLER PARAMETERS FOR "NORMAL WALKING": $k^*_{d()}$ (IN NEWTON·METERS), $b^*_{d()}$ (IN NEWTON·METER·SECONDS, AND $\theta^*_{()}$ (IN DEGREES)

| States | $k_{d1}$ | $k^*_{d2}$ | $k^*_{d3}$ | $k^*_{d4}$ | $b_{d1}$ | $b^*_{d2}$ | $b^*_{d3}$ | $b^*_{d4}$ |
|---|---|---|---|---|---|---|---|---|
| 1 | 400 | 700 | 30 | 20 | 50 | 300 | 5 | 15 |
| 2 | 400 | 70 | 30 | 20 | 50 | 1 | 5 | 15 |
| 3 | 400 | 70 | 0 | 5 | 50 | 1 | 1 | 1 |
| 4 | 400 | 0 | 30 | 5 | 50 | 0 | 5 | 1 |

| States | 1 | 2 | 3 | 4 |
|---|---|---|---|---|
| $\theta_b$ | 87.5 | | | |
| $\theta^*_l$ | 68 | 122 | 122 | – |
| $\theta^*_a$ | 0 | 0 | 10 | 0 |

Given the independence of each leg, there is no guarantee that each leg is fully out of phase with the other. Recall, however, that the control philosophy in this paper is to impose a minimum number of constraints and, thus, encourage the natural dynamics of the biped rather than constraining them. This is in contrast to an implementation that utilizes time-based switching, such as that described in [45]. Specifically, state switching happens along changes in constraint configuration that is initiated by the motion of the robot autonomously. Similar approach on a point foot robot and curved foot robot can be found in [21], [23], and [26], respectively.

### B. Simulation

For the biped illustrated in Fig. 1, the associated geometric and inertial parameters that are normalized to a body height $L$ and mass $M$, as given in [46], are listed in Table I. For purposes of control implementation and simulation, the biped was parameterized according to the values listed in Table I using a height $L = 1.8$ m and a mass $M = 75$ kg. The simulation was conducted by utilizing the desired generalized control force described in (16) and (17) and by using the actuator torque solution (15). The controller was parameterized by starting with initial estimates (guided by the characteristic times that typify human gait) and using the simulation to iteratively tune parameters for a robust and human-like gait. Specifically, control parameters were considered to be a robust set when the biped would, within a few steps, converge to a stable, natural-looking gait after starting from rest in several different initial configurations (e.g., double support with both feet flat, double support with only forward heel and backward toe in contact, and single support with foot flat).

Note that some type of automated parameter tuning could also be implemented for control gain selection. Due to the nonlinear character and nonsmooth nature of the problem, however, such automated parameter tuning is a nontrivial task that often requires additional hand tuning to provide a robust parameter set [45]. As such, for the simulations presented here, the control parameters were selected by hand-tuning and intuition.

*1) Dynamic Walking of the Biped:* For the (adult) human-scale anthropomorphic biped, the control parameters used for an approximately normal walking speed are listed in Table II (where the upper index $(*) = r/l$ represents the right or left leg, respectively). A stroboscopic image of the motion results of this controller, which is simulated over a period of $t \in [0, 10]$ s, is shown in Fig. 4. The corresponding real-time video of the resulting gait is included in the supporting material. For the simulation shown, the initial configuration of the biped was (starting at rest) in the double-support phase, with the forward heel on the ground and the backward toe on the ground. The average forward walking speed for this simulation, after converging to a stable limit cycle, was 0.81 m/s.

As was outlined in the paper, the presented control approach is designed to leverage the natural dynamics of the biped. A direct consequence is that the simulated motions have natural human style. Beyond this qualitative characteristic, the efficiency of dynamic walking should be improved relative to a ZMP-based approach, since the former need not use significant energy to override the natural dynamics of the biped. The efficiency of gait can be characterized by the specific mechanical cost of transport $c_{mt}$ = (mechanical energy)/(weight $\times$ distance traveled), which is adapted from the specific resistance, as presented in [47]. Based on the simulation shown in Fig. 4, the calculated mechanical cost of transport of the proposed approach is $c_{mt} = 0.19$. Comparatively, the specific mechanical cost of transport of the ZMP-based Honda Asimo is *estimated* as $c_{mt} = 1.6$ [14], while the cost of transport of the (actuator-assisted) Cornell dynamic walker is $c_{mt} = 0.05$ [14]. As such, the walking synthesized with the proposed approach, which presumably is (as subsequently demonstrated) more robust and versatile than an actuator-assisted approach, can also be nearly an order of magnitude more efficient than walking generated by trajectory-tracking approaches.

*2) Walking With Different Speeds:* In order to demonstrate versatility in the control approach, simulations were also conducted for faster and slower walking speeds. Multiple possibilities exist for varying the control parameter set to achieve stable locomotion with different walking speeds. An intuitive parameter that can be varied to influence the walking speed is the hip stiffness during stance (i.e., $k_{d2}$ in state 1), which affects the leg dynamics with respect to the inertial frame. Figs. 5 and 6 show stroboscopic images of the biped walking at faster and slower walking speeds (relative to Fig. 4), respectively, both simulated over a period of $t \in [0, 10]$ s and generated by utilizing the same control parameter set that is given in Table II but with different values of the stance hip stiffness. Specifically, to achieve these gaits, the corresponding stiffness value was set to $k_{d2} = 800$ N·m and $k_{d2} = 600$ N·m, respectively. The faster gait, which is shown in Fig. 5 starting from rest at an initial condition of double support with both feet flat on the ground, is characterized by an average walking

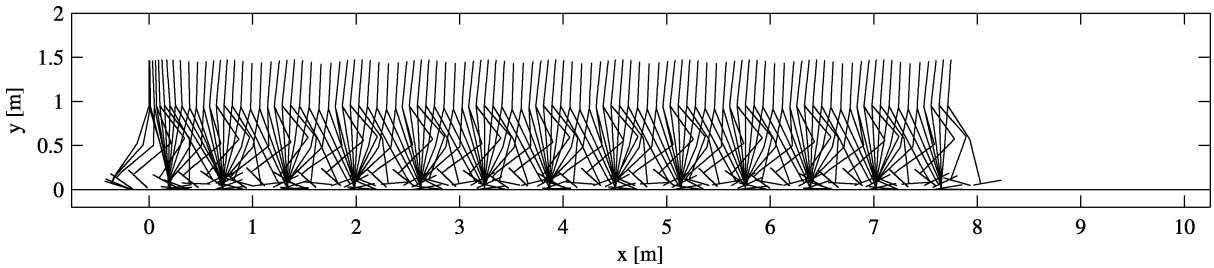


Fig. 4. Stroboscopic view of dynamic walking with 0.81 m/s average forward speed. The motion is started from double-support phase, while only the forward heel and the backward toe are on the ground: $\mathbf{q}(0) = [0, 1.27, 1.57, 1.82, 1.78, 0.2, 1.31, 1.04, -0.35]^T$, $\dot{\mathbf{q}}(0) = \mathbf{0}$. The calculated specific cost of transport is $c_{mt} = 0.19$. Within a cycle, the walker spent $15.6\%$ in double-support phase.

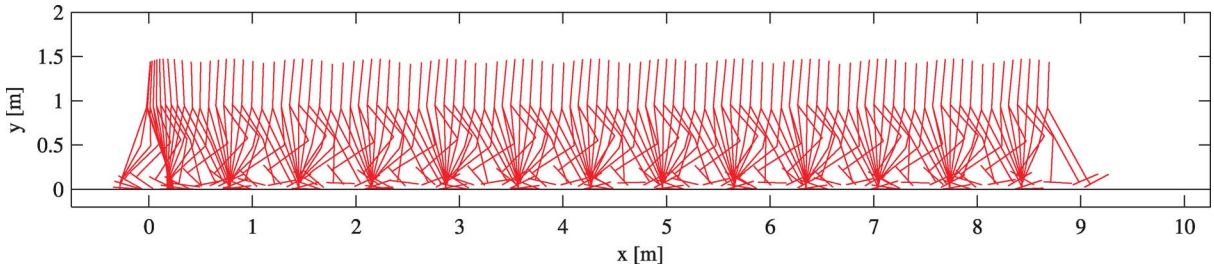


Fig. 5. Stroboscopic view of dynamic walking with 0.92 m/s average forward speed. The motion is started from double support with both feet flat on the ground: $\mathbf{q}(0) = [0, 1.24, 1.5, 1.86, 1.86, 0, 1.23, 1.23, 0]^T$, $\dot{\mathbf{q}}(0) = \mathbf{0}$. The calculated specific cost of transport is $c_{mt} = 0.22$. Within a cycle, the walker spent $16\%$ in double-support phase.

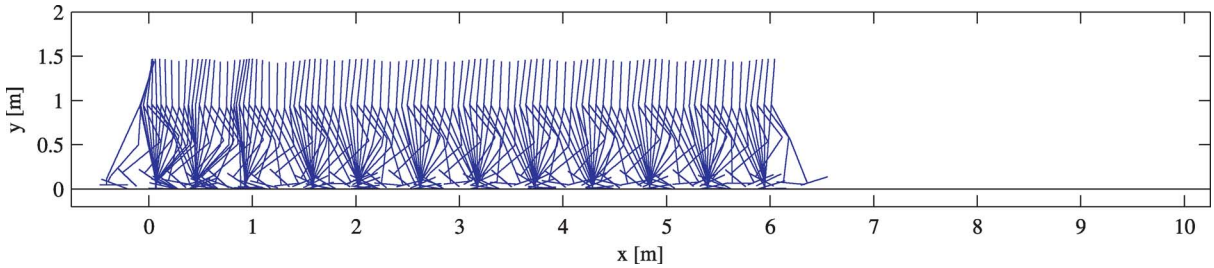


Fig. 6. Stroboscopic view of dynamic walking with 0.68 m/s average forward speed. The motion is started from single support with the forward foot flat on the ground: $\mathbf{q}(0) = [0, 1.25, 1.3, 1.75, 1.75, 0, 1.2, 1.2, 0]^T$, $\dot{\mathbf{q}}(0) = \mathbf{0}$. The calculated specific cost of transport is $c_{mt} = 0.17$. Within a cycle, the walker spent $18.3\%$ in double support.

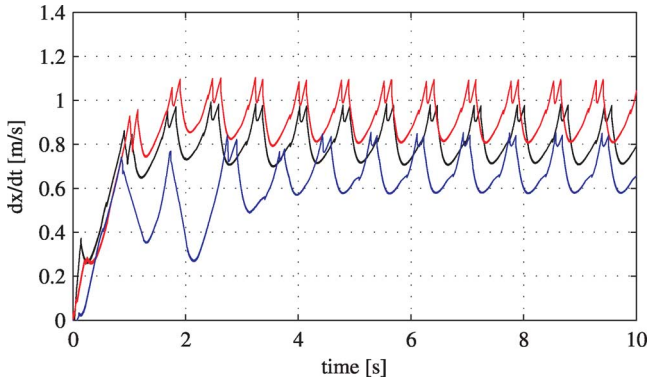


Fig. 7. Forward velocity of the upper body CoM for walking at three different speeds. The average velocities $\dot{x}_{\text{avg}} = [0.92, 0.81, 0.68]$ m/s are calculated on the sustained walking cycles by $\dot{x}_{\text{avg}} = \int_{T_1}^{T_2} \dot{x}(t)dt/(T_2 - T_1)$, where $T_1 = 5$ s, and $T_2 = 10$ s.

speed of 0.92 m/s. The slower gait, which is shown in Fig. 6 starting from rest at an initial condition of single support with the foot flat on the ground, is characterized by an average walking speed of 0.68 m/s. Corresponding real-time videos of these simulations are included in the supporting material.

Fig. 7 shows the respective forward velocities (of the center of mass of the torso) at each of the three walking speeds. The time evolution of the upper body angle for the three gaits are depicted in Fig. 8. As can be seen in the figure, the torso for each case starts at an upper body posture away from the limit cycle and, in each case, converges within a few steps to a stable limit cycle. Fig. 9 shows the phase plane plots for the (right-side) hip, knee, and ankle joints, for each of the three gaits, which clearly indicates that a stable limit cycle has been reached in each case. The fact that the biped achieves a stable limit cycle within a few steps for several different walking speeds from different initial conditions by varying only a single control parameter (i.e., hip stiffness during stance $k_{d2}$) is demonstrative of the ability of the method to generate walking with different speeds and shows robustness with respect to variation in initial conditions. Different control parameters, such as the upper body angle $\theta_b$, hip damping at stance ($b^*_{d2}$ in state 1), and ankle stiffness in stance ($k^*_{d4}$ in states 1 and 2), can also be used to change the

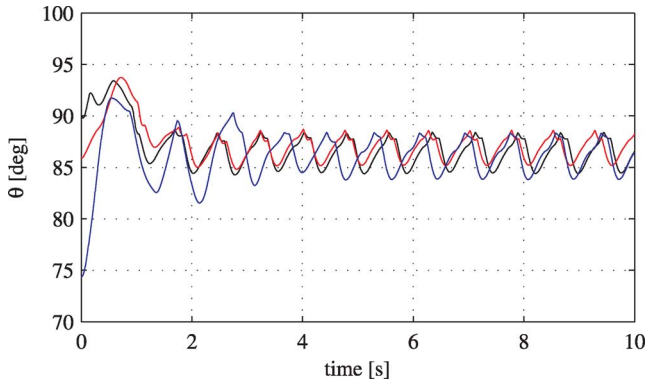


Fig. 8. Upper body angle during walking at three different speeds. The vertical upright position corresponds to $90^\circ$.

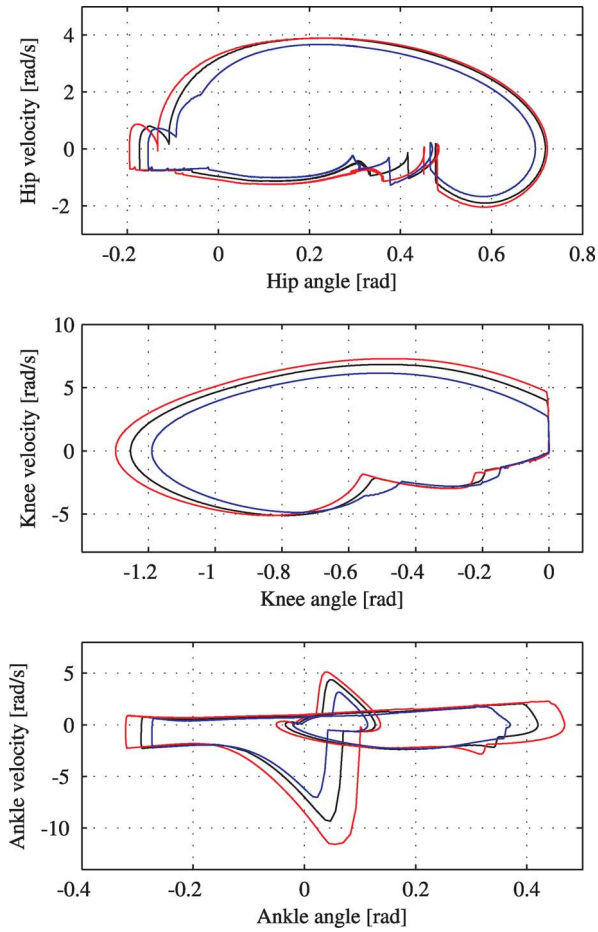


Fig. 9. Steady walking cycle for three different speeds for the (right) hip, knee, and ankle motion, respectively. The joint angles are defined as $\theta_1 - \theta$ for the hip, $\theta_2 - \theta_1$ for the knee, and $\theta_3 - \theta_2 + \pi/2$ for the ankle.

walking speed. While the proposed approach can also be used to make the robot stand, natural-looking walking was obtained in a speed range of $[0.6, 1.2]$ m/s.

*3) Walking With Different Style:* In order to illustrate the differing character of gait achieved with a different set of control parameters, the biped was simulated with the set of control parameters that are listed in Table III. The stroboscopic image

TABLE III
CONTROLLER PARAMETERS: $k^*_{d()}$ (IN NEWTON·METERS), $b^*_{d()}$ (IN NEWTON·METER·SECONDS), AND $\theta^*_{()}$ (IN DEGREES)

| States | $k_{d1}$ | $k^*_{d2}$ | $k^*_{d3}$ | $k^*_{d4}$ | $b_{d1}$ | $b^*_{d2}$ | $b^*_{d3}$ | $b^*_{d4}$ |
|---|---|---|---|---|---|---|---|---|
| 1 | 500 | 750 | 40 | 10 | 35 | 250 | 3 | 10 |
| 2 | 500 | 65 | 40 | 10 | 35 | 1.5 | 3 | 10 |
| 3 | 500 | 65 | 0 | 5 | 35 | 1.5 | 1.25 | 2 |
| 4 | 500 | 0 | 40 | 5 | 35 | 0 | 3 | 2 |

| States | 1 | 2 | 3 | 4 |
|---|---|---|---|---|
| $\theta_b$ | 84 | | | |
| $\theta^*_l$ | 67 | 125 | 125 | – |
| $\theta^*_a$ | 0 | 0 | 5 | 0 |

of walking with this controller, which is simulated over a period of $t \in [0, 10]$ s and corresponds to an initial condition of starting at rest in double support with the forward heel on the ground and the backward toe on the ground, is shown in Fig. 10. The corresponding real-time video of the resulting gait is included in the supporting material. The differing character of gait is evident by comparing the video that corresponds to Fig. 10 with the video that corresponds to the gait depicted in Fig. 4. The motion that is obtained under substantial variation in control parameters also demonstrates robustness with respect to control parameter variation.

Based on our experience with simulation of the biped, stable walking is achievable with a relatively large range of control parameters. Differing sets of control parameters result in a differing character of gait, some of which appear more natural and efficient than others. Other sets of parameters generate gaits that appear either more relaxed or more deliberate. There also obviously exists a large space of parameters that fail. A video of one such failure is included in the supplemental material. This particular failure is due to a "weak" gait (caused by hip torques that do not generate sufficiently large steps) that ultimately results in a stumble.

*4) Push Disturbance Response:* In order to demonstrate robustness to push-type disturbances, the biped was simulated at the three speeds with impulsive forward and backward push-type disturbances. Specifically, an impulsive force was applied via a constant horizontal force of 200 N for a duration of 0.2 s, which is applied at the center of mass of the upper body in both the forward and backward directions, respectively. Note that these disturbances are similar to those described in [48]. In the six simulations (forward and backward pushes at three different speeds), the robot recovered fully in all cases. In Fig. 11, all six push recovery test results are depicted. The corresponding real-time videos that are included in the supporting material demonstrate the push-type disturbance rejection of the proposed approach.

*5) Model Parameter Uncertainties:* Since the proposed approach is model-based, the authors further conducted numerical experiments to explore robustness with respect to model parameter variations. Specifically, 100 simulations were conducted, in which the mass matrix $\mathbf{M}$ and constraint matrix $\mathbf{A}$ that are used in the controller (15) were simultaneously varied element-wise by an average of $10\%$ relative to the exact values (used in the

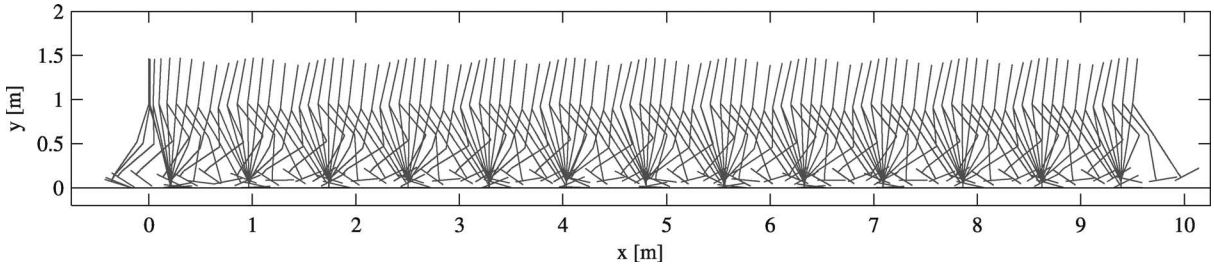


Fig. 10. Stroboscopic view of dynamic walking with 0.97 m/s average forward speed, which is simulated using the control parameters from Table III. The motion is started from double-support phase, while only the forward heel and the backward toe are on the ground: $\mathbf{q}(0) = [0, 1.27, 1.57, 1.82, 1.78, 0.2, 1.31, 1.04, -0.35]^T$, $\dot{\mathbf{q}}(0) = \mathbf{0}$.

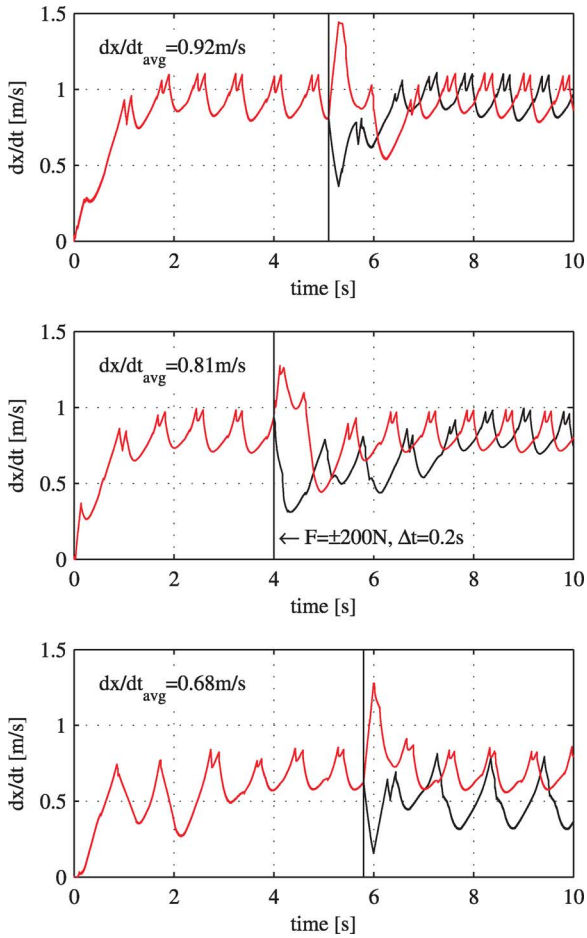


Fig. 11. Push experiment for the walk at $[0.92, 0.81, 0.68]$ m/s average speeds. The six separate experiments shown characterize the response to forward and backward pushes at $[5.1, 4, 5.8]$ s with 200 N force for a duration of 0.2 s, which act horizontally on the center of the upper body. While the walk remained stable in all six cases, at the slowest speed, the robot converged to a different cyclic trajectory after the forward push. Although the recovery time, in some cases, may seem long, the corresponding real-time video indicates a natural looking response.

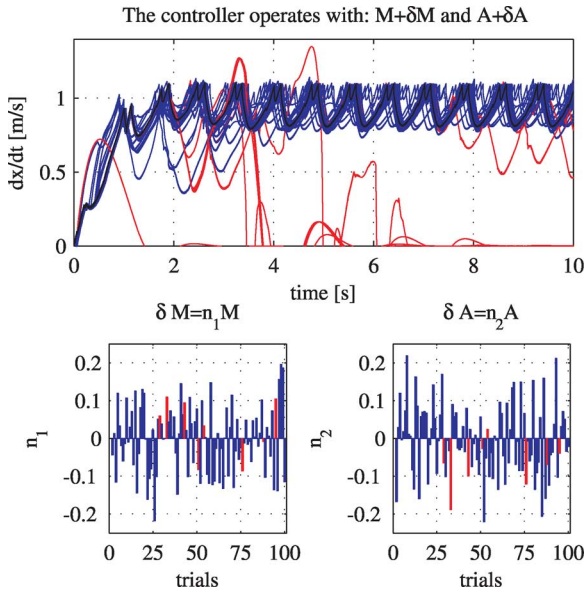


Fig. 12. Forward velocity versus time in 100 simulations under simultaneous variation of the mass matrix and constraint matrix. The random variables $n_{1,2}$ that are used to generate the parameter variation have normal distribution $N(\mu, \sigma^2)$ (with zero mean $\mu = 0$ and $\sigma = 0.1$ standard deviation). During the simulations, the robot remained stable in 92 trials, while it fell eight times (all during the starting steps).

dynamic model). As depicted in Fig. 12, the controller maintains stability with uncertainty in parameters, thus demonstrating a moderate degree of robustness to model parameter uncertainty.

*6) Walking on Slopes:* The versatility and robustness of the proposed approach was also explored by walking up and down slopes. In order to walk up and down slopes, four intuitive controller parameters were modified. Specifically, relative to the fast walking set of parameters, the following changes were made: The upper body angle was selected to be $\theta_b = \{80°, 90°\}$ (for the uphill and downhill walks, respectively), the equilibrium angle for the ankles at swing were changed to $\theta_a = 15°$ (to prevent stumbling), the hip-extension angle was $\theta_l = 128°$, and the knee stiffness at stance was changed to $k_{d3} = 50$ N·m. The corresponding simulation result for $\pm 5°$ upward and downward slopes are shown in Figs. 13 and 14. Real-time videos of the respective motions are included in the supporting material. Note that with the same parameters, the biped can also walk on level ground.

*7) Comment on 3-D Extension and Parameter Adaptation:* It should be noted that the approach presented herein considers sagittal plane motion, although extension to 3-D walking would neither change the structure of the model nor the control approach. Particularly, the walking controller would need to be extended with additional spring–damper elements that

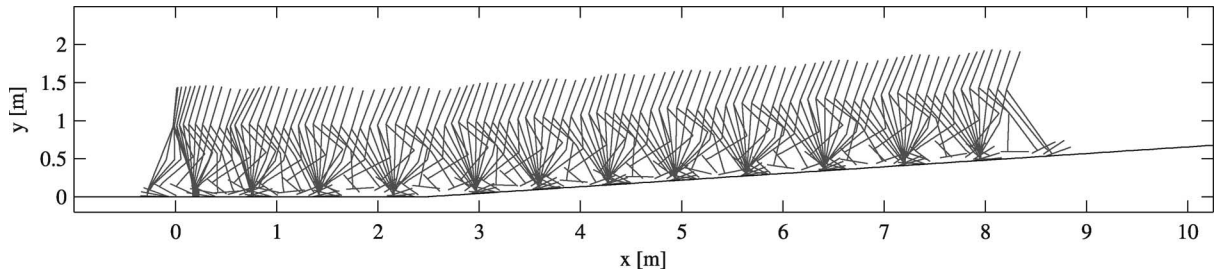


Fig. 13. Stroboscopic view of uphill walking, which is simulated using the control parameters from Table III. The motion is started from double support with both feet flat on the ground: $\mathbf{q}(0) = [0, 1.24, 1.5, 1.86, 1.86, 0, 1.23, 1.23, 0]^T$, $\dot{\mathbf{q}}(0) = \mathbf{0}$.

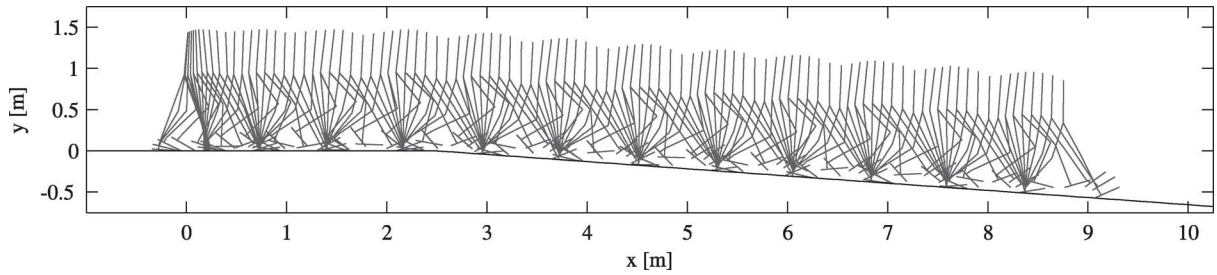


Fig. 14. Stroboscopic view of downhill walking, which is simulated using the control parameters from Table III. The motion is started from double support with both feet flat on the ground: $\mathbf{q}(0) = [0, 1.24, 1.5, 1.86, 1.86, 0, 1.23, 1.23, 0]^T$, $\dot{\mathbf{q}}(0) = \mathbf{0}$.

would apply a stabilizing torque to the (upper) body motion in the frontal plane relative to the IRF. Realization of the corresponding torques would be enabled with additional (hip and/or ankle) actuators on the robot. Finally, further implementation of parameter adaptation using learning techniques [26], although not explored here, may improve the inherent robustness of the approach that is demonstrated through numerous simulation results.

## V. Conclusion

The authors have proposed an approach for the control of biped walking that enables dynamic walking in a fully actuated biped robot. Rather than prescribing kinematic trajectories or kinematic constraints, the approach is based on the prescription of state-dependent torques that are obtained with low-gain spring–damper couples that "encourage" patterned movement through the natural dynamics of the biped. These simple set of torques are proposed that generate a stable gait, while this allows the biped to exploit its natural dynamics. Some of the prescribed torques are referenced to the IRF, which simplifies the selection and tuning of the control parameters. Implementation of torques from a mixed set of coordinate frames is enabled by a joint torque computation (based on Gauss's principle of least constraint), which is valid for all configurations of the biped. The proposed approach is implemented in simulation on an anthropomorphic biped, whose motion is shown to quickly converge to a natural looking gait limit cycle. Simulations are conducted with various control parameters, as well as different initial conditions. The mechanical cost of transport is calculated and shown to be nearly an order of magnitude lower than what would be expected from trajectory-tracking approaches. The authors additionally demonstrate versatility with respect to varying walking speeds and ground slopes, as well as robustness with respect to push-type disturbances and uncertainty in model parameters. Future work includes experimental implementation of the proposed approach.

## References

[1] M. Vukobratović and J. Stepanenko, "On the stability of antropometric systems," *Math. Biosci.*, vol. 15, no. 1, pp. 1–37, 1972.
[2] M. Vukobratović, B. Borovac, D. Šurla, and D. Stokić, *Biped Locomotion*. New York: Springer-Verlag, 1990.
[3] K. Hirai, M. Hirose, Y. Haikawa, and T. Takenaka, "The development of Honda humanoid robot," in *Proc. IEEE ICRA*, 1998, pp. 1321–1326.
[4] Q. Huang, K. Yokoi, S. Kajita, K. Kaneko, H. Arai, N. Koyachi, and K. Tanie, "Planning walking patterns for a biped robot," *IEEE Trans. Robot. Autom.*, vol. 17, no. 3, pp. 280–289, Jun. 2001.
[5] S. Kagami, T. Kitagawa, K. Nishiwaki, T. Sugihara, M. Inaba, and H. Inoue, "A fast dynamically equilibrated walking trajectory generation method of humanoid robot," *Auton. Robots*, vol. 12, pp. 71–82, 2002.
[6] C. Chevallereau, D. Djoudi, and J. W. Grizzle, "Stable bipedal walking with foot rotation through direct regulation of the zero moment point," *IEEE Trans. Robot.*, vol. 24, no. 2, pp. 390–401, Apr. 2008.
[7] A. D. Kuo, "Choosing your steps carefully," *IEEE Robot. Autom. Mag.*, vol. 14, no. 2, pp. 18–29, Jun. 2007.
[8] M. Garcia, A. Ruina, A. Chatterjee, and M. Coleman, "The simplest walking model: Stability, complexity, and scaling," *J. Biomech. Eng.*, vol. 120, no. 2, pp. 281–288, 1998.
[9] S. Mochon and T. A. McMahon, "Ballistic walking: An improved model," *Math. Biosci.*, vol. 52, pp. 241–260, 1980.
[10] C.-L. Shih, "The dynamics and control of a biped walking robot with seven degrees of freedom," *J. Dyn. Syst., Meas., Control*, vol. 118, no. 4, pp. 683–690, 1996.
[11] A. Goswami, "Postural stability of biped robots and the foot-rotation indicator (FRI) point," *Int. J. Robot. Res.*, vol. 18, pp. 523–533, 1999.
[12] T. McGeer, "Passive dynamic walking," *Int. J. Robot. Res.*, vol. 9, no. 2, pp. 2–62, 1990.
[13] M. J. Coleman and A. Ruina, "An uncontrolled walking toy that cannot stand still," *Phys. Rev. Lett.*, vol. 80, no. 16, pp. 16–3658, 1998.
[14] S. Collins, A. Ruina, R. Tedrake, and M. Wisse, "Efficient bipedal robots based on passive dynamic walkers," *Sci. Mag.*, vol. 307, pp. 1082–1085, 2005.

[15] M. Wisse, G. Feliksdal, J. van Frankenhuyzen, and B. Moyer, "Passive-based walking robot: Denis, a simple efficient and lightweight biped," *IEEE Robot. Autom. Mag.*, vol. 14, no. 2, pp. 52–62, Jun. 2007.
[16] F. Iida, Y. Minekawa, J. Rummel, and A. Seyfarth, "Toward a human-like biped robot with compliant legs," *Robot. Auton. Syst.*, vol. 52, pp. 139–144, 2009.
[17] H. Geyer, A. Seyfarth, and R. Blickhan, "Compliant leg behaviour explains basic dynamics of walking and running," *Proc. R. Soc. Lond. B*, vol. 273, pp. 2861–2867, 2006.
[18] J. W. Grizzle, G. Abba, and F. Plestan, "Asymptotically stable walking for biped robots: Analysis via systems with impulse effects," *IEEE Trans. Autom. Control*, vol. 46, no. 1, pp. 51–64, Jan. 2001.
[19] F. Plestan, J. W. Grizzle, E. R. Westervelt, and G. Abba, "Stable walking of a 7-dof biped robot," *IEEE Trans. Robot. Autom.*, vol. 19, no. 4, pp. 653–668, Aug. 2003.
[20] E. R. Westervelt, J. W. Grizzle, and D. E. Koditschek, "Hybrid zero dynamics of planar biped walkers," *IEEE Trans. Autom. Control*, vol. 48, no. 1, pp. 42–56, Jan. 2003.
[21] C. Chevallereau, G. Abba, Y. Aoustin, F. Plestan, E. Westervelt, C. de Wit, and J. Grizzle, "RABBIT: A testbed for advanced control theory," *IEEE Control Syst. Mag.*, vol. 23, no. 5, pp. 57–79, Oct. 2003.
[22] C. C. de Wit, "On the concept of virtual constraints as a tool for walking robot control and balancing," *Annu. Rev. Control*, vol. 28, pp. 157–166, 2004.
[23] C. Sabourin and O. Bruneau, "Robustness of the dynamic walk of a biped robot subjected to disturbing external forces by using CMAC neural networks," *Robot. Auton. Syst.*, vol. 51, pp. 81–99, 2005.
[24] J. Pratt, C. M. Chew, A. Torres, P. Dilworth, and G. Pratt, "Virtual model control: An intuitive approach for bipedal locomotion," *Int. J. Robot. Res.*, vol. 20, pp. 129–143, 2001.
[25] T. Geng, B. Porr, and F. Wörgötter, "Fast biped walking with a sensor-driven neuronal controller and real-time online learning," *Int. J. Robot. Res.*, vol. 25, no. 3, pp. 3–243, 2006.
[26] P. Manoonpong, T. Geng, T. Kulvicius, B. Porr, and F. Wörgötter, "Adaptive, fast walking in a biped robot under neuronal control and learning," *PLoS Comput. Biol.*, vol. 3, no. 7, pp. 7–1305, 2007.
[27] C. F. Gauss, "Über ein neues algemeines grundgesetz der mechanik," *Z. die reine angew. Math.*, vol. 4, pp. 232–235, 1829.
[28] L. A. Pars, *A Treatise on Analytical Dynamics*. New York: Wiley, 1965.
[29] F. E. Udwadia and R. E. Kalaba, "A new perspective on constrained motion," *Proc. R. Soc. Lond. A*, vol. 439, pp. 407–410, 1992.
[30] H. Hemami and B. Wyman, "Modeling and control of constrained dynamic systems with application to biped locomotion in the frontal plane," *IEEE Trans. Autom. Control*, vol. AC-24, no. 4, pp. 526–535, Aug. 1979.
[31] W. Blajer and W. Schiehlen, "Walking without impacts as a motion/force control problem," *J. Dyn. Syst., Meas., Control*, vol. 114, pp. 660–665, 1992.
[32] F. E. Udwadia and R. E. Kalaba, *Analytical Dynamics: A New Approach*. Cambridge, U.K.: Cambridge Univ. Press, 1996.
[33] J. J. Moreau, "Quadratic programming in mechanics: Dynamics of one-sided constraints," *J. SIAM Control*, vol. 4, no. 1, pp. 1–153, 1966.
[34] Y. Hurmuzlu and D. Marghitu, "Multi-contact collisions of kinematic chains with external surfaces," *Int. J. Robot. Res.*, vol. 13, no. 1, pp. 1–82, 1994.
[35] B. Brogliato, *Nonsmooth Mechanics*, 2nd ed. London, U.K.: Springer-Verlag, 1999.
[36] B. Brogliato, A. A. ten Dam, L. Paoli, F. Génot, and M. Abadie, "Numerical simulation of finite dimensional multibody nonsmooth mechanical systems," *ASME Appl. Mech. Rev.*, vol. 55, no. 2, pp. 2–107, 2002.
[37] F. Pfeiffer and C. Glocker, *Multibody Dynamics With Unilateral Contacts*. New York: Wiley VCH, 1996.
[38] Y. Hurmuzlu, F. Génot, and B. Brogliato, "Modeling, stability and control of biped robots—A general framework," *Automatica*, vol. 40, no. 10, pp. 10–1647, 2004.
[39] L. Lilov and M. Lorer, "Dynamic analysis of multirigid-body system based on the Gauss principle," *Z. Angew. Math. Mech.*, vol. 62, pp. 539–545, 1982.
[40] G. Golub and C. V. Loan, *Matrix Computations*, 3rd ed. Baltimore, MD: Johns Hopkins Univ. Press, 1996.
[41] A. Ben Israel and T. N. E. Greville, *Generalized Inverse: Theory and Applications*. New York: Springer-Verlag, 2003.
[42] K. L. Doty, C. Melchiorri, and C. Bonivento, "A theory of generalized inverses applied to robotics," *Int. J. Robot. Res.*, vol. 12, no. 1, pp. 1–19, 1993.
[43] T. Sugihara and Y. Nakamura, "Whole-body cooperative balancing of humanoid robot using COG Jacobian," in *Proc. IEEE/RSJ Int. Conf. Intell. Robots Syst.*, 2002, vol. 3, pp. 2575–2580.
[44] S. Hyon, J. G. Hale, and G. Cheng, "Full-body compliant human–humanoid interaction: Balancing in the presence of unknown external forces," *IEEE Trans. Robot.*, vol. 23, no. 5, pp. 884–898, Oct. 2007.
[45] K. Yin, K. Loken, and M. van de Panne, "Simbicon: Simple biped locomotion control," *ACM Trans. Graph.*, vol. 26, no. 3, pp. 105-1–105-10, 2007.
[46] D. A. Winter, *Biomechanics and Motor Control of Human Movement*, 2nd ed. New York: Wiley–Interscience, 1990.
[47] G. Gabrielli and T. von Kármán, "What price speed?: Specific power required for propulsion of vehicles," *Mech. Eng.*, vol. 72, no. 10, pp. 775–781, 1950.
[48] A. Takanishi, T. Takeya, H. Karaki, and I. Kato, "A control method for dynamic biped walking under unknown external force," in *Proc. IEEE Int. Workshop Intell. Robots Syst.*, 1990, vol. 2, pp. 795–801.

**David J. Braun** (S'09) received the B.S. and M.S. degrees in mechanical engineering from the Faculty of Technical Sciences, University of Novi Sad, Novi Sad, Serbia, in 2001 and 2003, respectively. He is currently working toward the Ph.D. degree with the Department of Mechanical Engineering, Vanderbilt University, Nashville, TN.

His current research interests include modeling, simulation, and control of dynamical systems with application to walking robots.

**Michael Goldfarb** (S'93–M'95) received the B.S. degree in mechanical engineering from the University of Arizona, Tucson, in 1988 and the S.M. and Ph.D. degrees in mechanical engineering from the Massachusetts Institute of Technology, Cambridge, in 1992 and 1994, respectively.

In 1994, he joined the Department of Mechanical Engineering, Vanderbilt University, Nashville, TN, where he is currently a Professor. His research interests include the design and control of high-power-density actuators, control of fluid-powered actuators, the design and control of upper and lower extremity prostheses, restoration of gait to paralyzed persons, and control of bipedal locomotion.